1.5D Parallel Sparse Matrix-Vector Multiply

Enver Kayaaslan, Cevdet Aykanat, Bora Uçar

1.5D PARALLEL SPARSE MATRIX-VECTOR MULTIPLY*

ENVER KAYAASLAN†, CEVDET AYKANAT‡, AND BORA UÇAR§

Abstract. There are three common parallel sparse matrix-vector multiply algorithms: 1D row-parallel, 1D column-parallel and 2D row-column-parallel. The 1D parallel algorithms offer the advantage of having only one communication phase. On the other hand, the 2D parallel algorithm is more scalable but it suffers from two communication phases. Here, we introduce a novel concept of heterogeneous messages where a heterogeneous message may contain both input-vector entries and partially computed output-vector entries. This concept not only leads to a decreased number of messages, but also enables fusing the input- and output-communication phases into a single phase. These findings are exploited to propose a 1.5D parallel sparse matrix-vector multiply algorithm which is called local row-column-parallel. This proposed algorithm requires a constrained fine-grain partitioning in which each fine-grain task is assigned to the processor that contains either its input-vector entry, or its output-vector entry, or both. We propose two methods to carry out the constrained fine-grain partitioning. We conduct our experiments on a large set of test matrices to evaluate the partitioning qualities and partitioning times of these proposed 1.5D methods.

Key words. sparse matrix partitioning, parallel sparse matrix-vector multiplication, directed hypergraph model, bipartite vertex cover, combinatorial scientific computing

AMS subject classifications. 05C50, 05C65, 05C70, 65F10, 65F50, 65Y05

1. Introduction. Sparse matrix-vector multiply (SpMV) of the form $\mathbf{y} \leftarrow \mathbf{Ax}$ is a fundamental operation in many iterative solvers for linear systems, eigensystems and least squares problems. This renders the parallelization of SpMV operation an important problem. In the literature, there are three SpMV algorithms: *row-parallel*, *column-parallel*, and *row-column-parallel*. Row-parallel and column-parallel (called 1D) algorithms have a single communication phase, in which either the $\mathbf{x}$-vector or partial results on the $\mathbf{y}$-vector entries are communicated. Row-column-parallel (2D) algorithms have two communication phases; first the $\mathbf{x}$-vector entries are communicated, then the partial results on the y-vector entries are communicated. We propose another parallel SpMV algorithm in which both the $\mathbf{x}$-vector and the partial results on the $\mathbf{y}$-vector entries are communicated as in the 2D algorithms, yet the communication is handled in a single phase as in the 1D algorithms. That is why, the new parallel SpMV algorithm is dubbed 1.5D.

Partitioning methods based on graphs and hypergraphs are widely established to achieve 1D and 2D parallel algorithms. For 1D parallel SpMV, row-wise or column-wise partitioning methods are available. The scalability of 1D parallelism is limited especially when a row or a column has too many nonzeros in the row- and column-parallel algorithms, respectively. In such cases, the communication volume is high and the load balance is hard to achieve, severely reducing the solution space. The associated partitioning methods are usually the fastest alternatives. For 2D parallel SpMV, there are different partitioning methods. Among them, those that partition matrix entries individually, based on the fine-grain model [4], have the highest flexibility. That is why they usually obtain the lowest communication volume and achieve near perfect balance among nonzeros per processor [7]. However, the fine-grain partitioning approach usually results in higher number of messages; not surprisingly higher

*A preliminary version appeared in IPDPSW [12].

†NTENT, Inc., USA

‡Bilkent University, Turkey

§CNRS and LIP (UMR5668 CNRS-ENS Lyon-INRIA-UCBL), 46, allée d'Italie, ENS Lyon, Lyon, 69364, France.

number of messages hampers the parallel SpMV performance [11].

The parallel SpMV operation is composed of fine-grain tasks of multiply-and-add operations of the form $y_i \leftarrow y_i + a_{ij}x_j$. Here, each fine-grain task is identified with a unique nonzero and assumed to be performed by the processor that holds the associated nonzero by the *owner-computes rule*. The proposed 1.5D parallel SpMV imposes a special condition on the operands of the fine-grain task $y_i \leftarrow y_i + a_{ij}x_j$: the processor that holds a_{ij} should also hold x_j or should be responsible for y_i (or both). The standard rowwise and columnwise partitioning algorithms for 1D parallel algorithms satisfy the condition, but they are too restrictive. The standard fine-grain partitioning approach does not necessarily satisfy the condition. Here we propose two methods for partitioning for 1.5D parallel SpMV. With the proposed partitioning methods, the overall 1.5D parallel SpMV algorithm inherits the important characteristics of 1D and 2D parallel SpMV and the associated partitioning methods. In particular, it has

- a single communication phase as in 1D parallel SpMV,
- the partitioning flexibility close to that of 2D fine-grain partitioning,
- much reduced number of messages compared to the 2D fine-grain partitioning,
- a partitioning time close to that of 1D partitioning.

We propose two methods (Section 4) to obtain a 1.5D local fine-grain partition each with a different setting and approach where some preliminary studies on these methods are given in our recent work [12]. The first method is developed by proposing a directed hypergraph model. Since current partitioning tools cannot meet 1.5D partitioning requirements, we adopt and adapt an approach similar to that of a recent work by Pelt and Bisseling. [15]. The second method has two parts. The first part applies a conventional 1D partitioning method but decodes this only as a partition of the vectors x and y. The second part decides nonzero/task distribution under the fixed partition of the input and output vectors.

The remainder of this paper is as follows. In Section 2, we give a background on parallel SpMV. Section 3 presents the proposed 1.5D local row-column-parallel algorithm and 1.5D local fine-grain partitioning. The two methods proposed to obtain a local fine-grain partition are presented and discussed in Section 4. Section 5 gives a brief review of recent related work. We display our experimental results in Section 6 and conclude the paper in Section 7.

2. Background on parallel sparse matrix-vector multiply.

2.1. The anatomy of parallel sparse matrix-vector multiply. Recall that $\mathbf{y} \leftarrow \mathbf{Ax}$ can be cast as a collection of fine-grain tasks of multiply-and-add operations

$$y_i \leftarrow y_i + a_{ij} \times x_j \ . \tag{1}$$

These tasks can share input and output-vector entries. When a task a_{ij} and the input-vector entry x_j are assigned to different processors, say P_ℓ and P_r, respectively, P_r sends x_j to P_ℓ, which is responsible to carry out the task a_{ij}. An input-vector entry x_j is not communicated multiple times between processor pairs. When a task a_{ij} and the output-vector entry y_i are assigned to different processors, say P_r and P_k, respectively, then P_r performs $\hat{y}_i \leftarrow \hat{y}_i + a_{ij} \times x_j$ as well as all other multiply-and-add operations that contribute to the partial result $\hat{y}_i$ and then sends $\hat{y}_i$ to P_k. The partial results received by P_k from different processors are then summed to compute y_i.

2.2. Task-and-data distributions. Let $\mathbf{A}$ be an $m \times n$ sparse matrix and a_{ij} represent both a nonzero of $\mathbf{A}$ and the associated fine-grain task of multiply-and-add operation (1). Let $\mathbf{x}$ and $\mathbf{y}$ be the input- and output-vectors of size n and

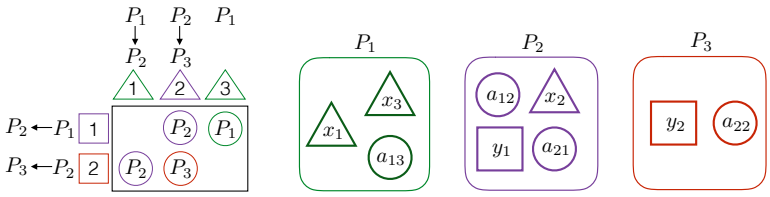

Fig. 1: A task-and-data distribution $\Pi(\mathbf{y} \leftarrow \mathbf{A}\mathbf{x})$ of matrix-vector multiply with a 2×3 sparse matrix $\mathbf{A}$.

m, respectively, and K be the number of processors. We define a K-way task-and-data distribution $\Pi(\mathbf{y} \leftarrow \mathbf{A}\mathbf{x})$ of the associated SpMV as a 3-tuple $\Pi(\mathbf{y} \leftarrow \mathbf{A}\mathbf{x}) = (\Pi(\mathbf{A}), \Pi(\mathbf{x}), \Pi(\mathbf{y}))$, where $\Pi(\mathbf{A}) = \{\mathbf{A}^{(1)}, \ldots, \mathbf{A}^{(K)}\}$, $\Pi(\mathbf{x}) = \{\mathbf{x}^{(1)}, \ldots, \mathbf{x}^{(K)}\}$, and $\Pi(\mathbf{y}) = \{\mathbf{y}^{(1)}, \ldots, \mathbf{y}^{(K)}\}$. We can also represent $\Pi(\mathbf{A})$ as a nonzero-disjoint summation

$$\mathbf{A} = \mathbf{A}^{(1)} + \mathbf{A}^{(2)} + \cdots + \mathbf{A}^{(K)}. \tag{2}$$

In $\Pi(\mathbf{x})$ and $\Pi(\mathbf{y})$, each $\mathbf{x}^{(k)}$ and $\mathbf{y}^{(k)}$ is a disjoint subvector of $\mathbf{x}$ and $\mathbf{y}$, respectively. Figure 1 illustrates a sample 3-way task-and-data distribution of matrix-vector multiply on a 2×3 sparse matrix.

For given input- and output-vector distributions $\Pi(\mathbf{x})$ and $\Pi(\mathbf{y})$, the columns and rows of $\mathbf{A}$ and those of $\mathbf{A}^{(k)}$ can be permuted, conformably with $\Pi(\mathbf{x})$ and $\Pi(\mathbf{y})$, to form $K \times K$ block structures:

$$\text{(3) } \mathbf{A} = \begin{bmatrix} \mathbf{A}_{11} & \mathbf{A}_{12} & \cdots & \mathbf{A}_{1K} \\ \mathbf{A}_{21} & \mathbf{A}_{22} & \cdots & \mathbf{A}_{2K} \\ \vdots & \vdots & \ddots & \vdots \\ \mathbf{A}_{K1} & \mathbf{A}_{K2} & \cdots & \mathbf{A}_{KK} \end{bmatrix}, \quad \text{(4) } \mathbf{A}^{(k)} = \begin{bmatrix} \mathbf{A}^{(k)}_{11} & \mathbf{A}^{(k)}_{12} & \cdots & \mathbf{A}^{(k)}_{1K} \\ \mathbf{A}^{(k)}_{21} & \mathbf{A}^{(k)}_{22} & \cdots & \mathbf{A}^{(k)}_{2K} \\ \vdots & \vdots & \ddots & \vdots \\ \mathbf{A}^{(k)}_{K1} & \mathbf{A}^{(k)}_{K2} & \cdots & \mathbf{A}^{(k)}_{KK} \end{bmatrix}.$$

Note that the row and column orderings (4) of the individual $\mathbf{A}^{(k)}$ matrices are in compliance with the row and column orderings (3) of $\mathbf{A}$. Hence, each block $\mathbf{A}_{k\ell}$ of the block structure (3) of $\mathbf{A}$ can be written as a nonzero-disjoint summation

$$\mathbf{A}_{k\ell} = \mathbf{A}^{(1)}_{k\ell} + \mathbf{A}^{(2)}_{k\ell} + \cdots + \mathbf{A}^{(K)}_{k\ell}. \tag{5}$$

Let $\Pi(\mathbf{y} \leftarrow \mathbf{A}\mathbf{x})$ be any K-way task-and-data distribution. According to this distribution, each processor P_k holds the submatrix $\mathbf{A}^{(k)}$, holds the input-subvector $\mathbf{x}^{(k)}$ and is responsible for storing/computing the output subvector $\mathbf{y}^{(k)}$. The fine-grain tasks (1) associated with the nonzeros of $\mathbf{A}^{(k)}$ are to be carried out by P_k. An input-vector entry $x_j \in \mathbf{x}^{(k)}$ is sent from P_k to P_ℓ, which is called an *input communication*, if there is a task $a_{ij} \in \mathbf{A}^{(\ell)}$ associated with a nonzero at column j. On the other hand, P_k receives a partial result $\hat{y}_i$ on an output-vector entry $y_i \in \mathbf{y}^{(k)}$ from P_ℓ, which is referred to as an *output communication*, if there is a task $a_{ij} \in \mathbf{A}^{(\ell)}$ associated with a nonzero at row i. Therefore, the fine-grain tasks associated with the nonzeros of the column stripe $\mathbf{A}_{*k} = [\mathbf{A}^T_{1k}, \ldots, \mathbf{A}^T_{Kk}]^T$ are the only ones that require an input-vector entry of $\mathbf{x}^{(k)}$ and the fine-grain tasks associated with the nonzeros of the row stripe $\mathbf{A}_{k*} = [\mathbf{A}_{k1}, \ldots, \mathbf{A}_{kK}]$ are the only ones that contribute to the computation of an output-vector entry of $\mathbf{y}^{(k)}$.

2.3. 1D parallel sparse matrix-vector multiply. There are two main alternatives for 1D parallel SpMV, row-parallel and column-parallel.

In the row-parallel SpMV, the basic computational units are the rows. For an output-vector entry y_i assigned to processor P_k, the fine-grain tasks associated with the nonzeros of $\mathbf{A}_{i*} = \{a_{ij} \in \mathbf{A} : 1 \leq j \leq n\}$ are combined into a composite task of inner product $y_i \leftarrow \mathbf{A}_{i*}\mathbf{x}$ which is to be carried out by P_k. Therefore, for the row-parallel algorithm, a task-and-data distribution $\Pi(\mathbf{y} \leftarrow \mathbf{A}\mathbf{x})$ of matrix-vector multiply on $\mathbf{A}$ should satisfy the following condition:

$$a_{ij} \in \mathbf{A}^{(k)} \text{ whenever } y_i \in \mathbf{y}^{(k)} \ . \tag{6}$$

Then, $\Pi(\mathbf{A})$ coincides with the output-vector distribution $\Pi(\mathbf{y})$—each submatrix is a row stripe of the block structure (3) of $\mathbf{A}$. In the row-parallel parallel SpMV, all messages are communicated in an input-communication phase called *expand* where each message contains only input-vector entries.

In the column-parallel SpMV, the basic computational units are the columns. For an input-vector entry x_j assigned to processor P_k, the fine-grain tasks associated with the nonzeros of $\mathbf{A}_{*j} = \{a_{ij} \in \mathbf{A} : 1 \leq i \leq m\}$ are combined into a composite task of "daxpy" operation $\hat{\mathbf{y}}_k \leftarrow \hat{\mathbf{y}}_k + \mathbf{A}_{*j}x_j$ which is to be carried out by P_k where $\hat{\mathbf{y}}_k$ is the partially computed output-vector of P_k. As a result, a task-and-data distribution $\Pi(\mathbf{y} \leftarrow \mathbf{A}\mathbf{x})$ of matrix-vector multiply on $\mathbf{A}$ for the column-parallel algorithm should satisfy the following condition:

$$a_{ij} \in \mathbf{A}^{(k)} \text{ whenever } x_j \in \mathbf{x}^{(k)} \ . \tag{7}$$

Here, $\Pi(\mathbf{A})$ coincides with the input-vector distribution $\Pi(\mathbf{x})$—each submatrix $\mathbf{A}^{(k)}$ is a column stripe of the block structure (3) of $\mathbf{A}$. In the column-parallel SpMV, all messages are communicated in an output-communication phase called *fold* where each message contains only partially computed output-vector entries.

The column-net and row-net hypergraph models [3] can be respectively used to obtain the required task-and-data partitioning for the row-parallel and column-parallel SpMV.

2.4. 2D parallel sparse matrix-vector multiply. In the 2D parallel SpMV, also referred to as the row-column-parallel, the basic computational units are nonzeros [4, 7]. The row-column-parallel algorithm requires fine-grain partitioning which imposes no restriction on distributing tasks and data. The row-column-parallel algorithm contains two communication and two computational phases in an interleaved manner as shown in Algorithm 1. The algorithm starts with the expand phase where the required input-subvector entries are communicated. The second step computes only those partial results that are to be communicated in the following fold phase. In the final step, each processor computes its own output-subvector. If we have a rowwise partitioning, the steps 2, 3 and 4c are not needed and hence the algorithm reduces to the row-parallel algorithm. Similarly, the algorithm without steps 1, 2b and 4b, can be used when we have a columnwise partitioning. The row-column-net hypergraph model [4, 7] can be used to obtain the required task-and-data partitioning for row-column-parallel SpMV.

3. 1.5D parallel sparse matrix-vector multiply. In this section, we propose the local row-column-parallel SpMV algorithm that exhibits 1.5D parallelism. The proposed algorithm simplifies the row-column-parallel algorithm by combining the two communication phases into a single expand-fold phase while attaining a flexibility on nonzero/task distribution close to the flexibility attained by the row-column-parallel algorithm.

Algorithm 1 The row-column-parallel sparse matrix-vector multiply

For each processor P_k:

1. (*expand*) for each nonzero column stripe $\mathbf{A}_{*k}^{(\ell)}$, where $\ell \neq k$;
   (a) form vector $\hat{\mathbf{x}}_{\ell}^{(k)}$ which contains only those entries of $\mathbf{x}^{(k)}$ corresponding to nonzero columns in $\mathbf{A}_{*k}^{(\ell)}$ and
   (b) send vector $\hat{\mathbf{x}}_{\ell}^{(k)}$ to P_{ℓ},
2. for each nonzero row stripe $\mathbf{A}_{\ell *}^{(k)}$, where $\ell \neq k$; compute
   (a) $\mathbf{y}_k^{(\ell)} \leftarrow \mathbf{A}_{\ell k}^{(k)} \mathbf{x}^{(k)}$ and
   (b) $\mathbf{y}_k^{(\ell)} \leftarrow \mathbf{y}_k^{(\ell)} + \sum_{r \neq k} \mathbf{A}_{\ell r}^{(k)} \hat{\mathbf{x}}_k^{(r)}$
3. (*fold*) for each nonzero row stripe $\mathbf{A}_{\ell *}^{(k)}$, where $\ell \neq k$;
   (a) form vector $\hat{\mathbf{y}}_k^{(\ell)}$ which contains only those entries of $\mathbf{y}_k^{(\ell)}$ corresponding to nonzero rows in $\mathbf{A}_{\ell *}^{(k)}$ and
   (b) send vector $\hat{\mathbf{y}}_k^{(\ell)}$ to P_{ℓ},
4. compute output-subvector
   (a) $\mathbf{y}^{(k)} \leftarrow \mathbf{A}_{kk}^{(k)} \mathbf{x}^{(k)}$,
   (b) $\mathbf{y}^{(k)} \leftarrow \mathbf{y}^{(k)} + \mathbf{A}_{k\ell}^{(k)} \hat{\mathbf{x}}_k^{(\ell)}$ and
   (c) $\mathbf{y}^{(k)} \leftarrow \mathbf{y}^{(k)} + \sum_{\ell \neq k} \hat{\mathbf{y}}_{\ell}^{(k)}$.

In the well-known parallel SpMV, the messages are homogenous in the sense that they pertain to either $\mathbf{x}$- or $\mathbf{y}$-vector entries. In the proposed row-column-parallel SpMV algorithm, the number of messages are reduced with respect to the row-column-parallel algorithm by making the messages heterogenous (pertaining to both $\mathbf{x}$- and $\mathbf{y}$-vector entries), and by communicating them in a single expand-fold phase. If a processor P_{ℓ} sends a message to processor P_k in both of the expand and fold phases, then the number of messages required from P_{ℓ} to P_k reduces from two to one. However, if a message from P_{ℓ} to P_k is sent only in the expand phase or only in the fold phase, then there is no reduction in the number of such messages.

3.1. A Task categorization. We introduce a two-way categorization of input- and output-vector entries and a four-way categorization of fine-grain tasks (1) according to a task-and-data distribution $\Pi(\mathbf{y} \leftarrow \mathbf{A}\mathbf{x})$ of matrix-vector multiply on $\mathbf{A}$. For a task a_{ij}, the input-vector entry x_j is said to be *local* if both a_{ij} and x_j are assigned to the same processor; the output-vector entry y_i is said to be local if both a_{ij} and y_i are assigned to the same processor. With this definition, the tasks can be classified into four groups. The task

$$y_i \leftarrow y_i + a_{ij} \times x_j \text{ on } P_k \text{ is } \begin{cases} \text{input-output-local} & \text{if } x_j \in \mathbf{x}^{(k)} \text{ and } y_i \in \mathbf{y}^{(k)}, \\ \text{input-local} & \text{if } x_j \in \mathbf{x}^{(k)} \text{ and } y_i \notin \mathbf{y}^{(k)}, \\ \text{output-local} & \text{if } x_j \notin \mathbf{x}^{(k)} \text{ and } y_i \in \mathbf{y}^{(k)}, \\ \text{nonlocal} & \text{if } x_j \notin \mathbf{x}^{(k)} \text{ and } y_i \notin \mathbf{y}^{(k)}. \end{cases}$$

Recall that an input-vector entry $x_j \in \mathbf{x}^{(\ell)}$ is sent from P_{ℓ} to P_k if there exists a task $a_{ij} \in \mathbf{A}^{(k)}$ at column j, which implies that the task a_{ij} of P_k is either output-local or nonlocal since $x_j \notin \mathbf{x}^{(k)}$. Similarly, for an output-vector entry $y_i \in \mathbf{y}^{(\ell)}$, P_{ℓ} receives

a partial result $\hat{y}_i$ from P_k if a task $a_{ij} \in \mathbf{A}^{(k)}$, which implies that the task a_{ij} of P_k is either input-local or nonlocal since $y_i \notin \mathbf{y}^{(k)}$. We can also infer from that the input-output-local tasks neither depend on the input-communication phase nor incur a dependency on the output-communication phase. However, the nonlocal tasks are linked with both communication phases.

In the row-parallel algorithm, each of the fine-grain tasks is either input-output-local or output-local due to the rowwise partitioning condition (6). For this reason, no partial result is computed for other processors, and thus no output communication is incurred. In the column-parallel algorithm, each of the fine-grain tasks is either input-output-local or input-local due to the columnwise partitioning condition (7). In the row-column-parallel algorithm, the input and output communications have to be carried out in separate phases. The reason is that the partial results on the output-vector entries to be sent are partially derived by performing nonlocal tasks that rely on the input-vector entries received.

3.2. Local fine-grain partitioning. In order to remove the dependency between the two communication phases in the row-column-parallel algorithm, we propose the local fine-grain partitioning where "locality" refers to the fact that each fine-grain task is input-local, output-local or input-output-local. In other words, there is no nonlocal fine-grain task.

A task-and-data distribution $\Pi(\mathbf{y} \leftarrow \mathbf{A}\mathbf{x})$ of matrix-vector multiply on $\mathbf{A}$ is said to be a local fine-grain partition if the following condition is satisfied:

$$a_{ij} \in \mathbf{A}^{(k)} + \mathbf{A}^{(\ell)} \text{ whenever } y_i \in \mathbf{y}^{(k)} \text{ and } x_j \in \mathbf{x}^{(\ell)}. \tag{8}$$

Notice that this condition is equivalent to

$$\text{if } a_{ij} \in \mathbf{A}^{(k)} \text{ then either } x_j \in \mathbf{y}^{(k)}, \text{ or } y_i \in \mathbf{x}^{(k)}, \text{ or both.} \tag{9}$$

Due to (4) and (9), each submatrix $\mathbf{A}^{(k)}$ becomes of the following form

$$\mathbf{A}^{(k)} = \begin{bmatrix} 0 & \dots & \mathbf{A}^{(k)}_{1k} & \dots & 0 \\ \vdots & \ddots & \vdots & \ddots & \vdots \\ \mathbf{A}^{(k)}_{k1} & \dots & \mathbf{A}^{(k)}_{kk} & \dots & \mathbf{A}^{(k)}_{kK} \\ \vdots & \ddots & \vdots & \ddots & \vdots \\ 0 & \dots & \mathbf{A}^{(k)}_{Kk} & \dots & 0 \end{bmatrix}. \tag{10}$$

In this form, the tasks associated with the nonzeros of diagonal block $\mathbf{A}^{(k)}_{kk}$, the off-diagonal blocks of the row stripe $\mathbf{A}^{(k)}_{k*}$, and the off-diagonal blocks of the column-stripe $\mathbf{A}^{(k)}_{*k}$ are input-output-local, output-local and input-local, respectively. Furthermore, due to (5) and (8), each off-diagonal block $\mathbf{A}_{k\ell}$ of the block structure (3) induced by the vector distribution ($\Pi(\mathbf{x})$,$\Pi(\mathbf{y})$) becomes

$$\mathbf{A}_{k\ell} = \mathbf{A}^{(k)}_{k\ell} + \mathbf{A}^{(\ell)}_{k\ell}\ , \tag{11}$$

and for each diagonal block we have $\mathbf{A}_{kk} = \mathbf{A}^{(k)}_{kk}$.

In order to clarify Equations (8)–(11), we provide the following 4-way local fine-grain partition on $\mathbf{A}$ as permuted into a 4×4 block structure.

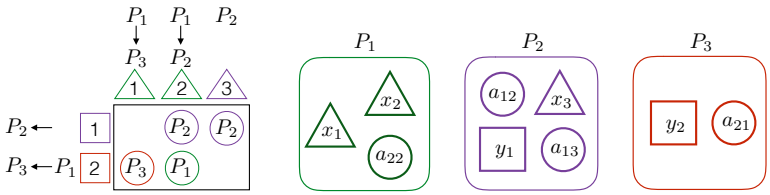

Fig. 2: A sample local fine-grain partition. Here, a_{12} is an output-local task, a_{13} is an input-output-local task, a_{21} is an output-local task, and a_{22} is an input-local task.

$$\mathbf{A} = \begin{bmatrix} \mathbf{A}_{11} & \mathbf{A}_{12}^{(1)} & \mathbf{A}_{13}^{(1)} & \mathbf{A}_{14}^{(1)} \\ \mathbf{A}_{21}^{(1)} & 0 & 0 & 0 \\ \mathbf{A}_{31}^{(1)} & 0 & 0 & 0 \\ \mathbf{A}_{41}^{(1)} & 0 & 0 & 0 \end{bmatrix} + \begin{bmatrix} 0 & \mathbf{A}_{12}^{(2)} & 0 & 0 \\ \mathbf{A}_{21}^{(2)} & \mathbf{A}_{22} & \mathbf{A}_{23}^{(2)} & \mathbf{A}_{24}^{(2)} \\ 0 & \mathbf{A}_{32}^{(2)} & 0 & 0 \\ 0 & \mathbf{A}_{42}^{(2)} & 0 & 0 \end{bmatrix} +$$

$$\begin{bmatrix} 0 & 0 & \mathbf{A}_{13}^{(3)} & 0 \\ 0 & 0 & \mathbf{A}_{23}^{(3)} & 0 \\ \mathbf{A}_{31}^{(3)} & \mathbf{A}_{32}^{(3)} & \mathbf{A}_{33} & \mathbf{A}_{34}^{(3)} \\ 0 & 0 & \mathbf{A}_{43}^{(3)} & 0 \end{bmatrix} + \begin{bmatrix} 0 & 0 & 0 & \mathbf{A}_{14}^{(4)} \\ 0 & 0 & 0 & \mathbf{A}_{24}^{(4)} \\ 0 & 0 & 0 & \mathbf{A}_{34}^{(4)} \\ \mathbf{A}_{41}^{(4)} & \mathbf{A}_{42}^{(4)} & \mathbf{A}_{43}^{(4)} & \mathbf{A}_{44} \end{bmatrix}.$$

For instance, $\mathbf{A}_{42} = \mathbf{A}_{42}^{(2)} + \mathbf{A}_{42}^{(4)}$, $\mathbf{A}_{23} = \mathbf{A}_{23}^{(2)} + \mathbf{A}_{23}^{(3)}$, $\mathbf{A}_{31} = \mathbf{A}_{31}^{(1)} + \mathbf{A}_{31}^{(3)}$, ..., etc.

Figure 2 displays a sample 3-way local fine-grain partition on the same sparse matrix used in Figure 1. In this figure, $a_{13} \in \mathbf{A}^{(1)}$ where $y_1 \in \mathbf{y}^{(2)}$ and $x_3 \in \mathbf{x}^{(1)}$ and thus a_{13} is an input-local task of P_1. Also, $a_{21} \in \mathbf{A}^{(3)}$ where $y_2 \in \mathbf{y}^{(3)}$ and $x_1 \in \mathbf{x}^{(1)}$ and thus a_{21} is an output-local task of P_3.

3.3. Local row-column-parallel sparse matrix-vector multiply. As there is no nonlocal tasks, the output-local tasks depend on input communication, and the output communication depends on the input-local tasks. Therefore, the tasks groups and communication phases can be arranged as: (i) input-local tasks; (ii) output-communication, input-communication; (iii) output-local tasks and input-output-local tasks. The input and output communication phases can be combined into the expand-fold phase, and the output-local and input-output-local task groups can be combined into a single computation phase to simplify the overall execution.

The local row-column-parallel algorithm is composed of three steps as shown in Algorithm 2. In the first step, processors concurrently perform their input-local tasks which contribute to partially computed output-vector entries for other processors. In the expand-fold phase, for each nonzero off-diagonal block $\mathbf{A}_{\ell k} = \mathbf{A}_{\ell k}^{(k)} + \mathbf{A}_{\ell k}^{(\ell)}$, P_k prepares a message $[\hat{\mathbf{x}}_\ell^{(k)}, \hat{\mathbf{y}}_k^{(\ell)}]$ for P_ℓ. Here, $\hat{\mathbf{x}}_\ell^{(k)}$ contains the input-vector entries of $\mathbf{x}^{(k)}$ that are required by the output-local tasks of P_ℓ, whereas $\hat{\mathbf{y}}_k^{(\ell)}$ contains the partial results on the output-vector entries of $\mathbf{y}^{(\ell)}$, where the partial results are derived by performing the input-local tasks of P_k. In the last step, each processor P_k computes output-subvector $\mathbf{y}^{(k)}$ by summing the partial results computed locally by its own input-output-local tasks (step 3a) and output-local tasks (step 3b) as well as the partial results received from other processors due to their input-local tasks (step 3c).

For a message $[\hat{\mathbf{x}}_\ell^{(k)}, \hat{\mathbf{y}}_k^{(\ell)}]$ from processor P_k to P_ℓ, the input-vector entries of $\hat{\mathbf{x}}_\ell^{(k)}$ correspond to the nonzero columns of $\mathbf{A}_{\ell k}^{(\ell)}$, whereas the partially computed output-

Algorithm 2 The local row-column-parallel sparse matrix-vector multiply

For each processor P_k:

1. for each nonzero block $\mathbf{A}^{(k)}_{\ell k}$, where $\ell \neq k$;
   compute $\mathbf{y}^{(\ell)}_k \leftarrow \mathbf{A}^{(k)}_{\ell k}\mathbf{x}^{(k)}$, ▶ input-local tasks of P_k
2. (*expand-fold*) for each nonzero block $\mathbf{A}_{\ell k} = \mathbf{A}^{(k)}_{\ell k} + \mathbf{A}^{(\ell)}_{\ell k}$, where $\ell \neq k$;
   (a) form vector $\hat{\mathbf{x}}^{(k)}_\ell$, which contains only those entries of $\mathbf{x}^{(k)}$ corresponding to nonzero columns in $\mathbf{A}^{(\ell)}_{\ell k}$,
   (b) form vector $\hat{\mathbf{y}}^{(\ell)}_k$, which contains only those entries of $\mathbf{y}^{(\ell)}_k$ corresponding to nonzero rows in $\mathbf{A}^{(k)}_{\ell k}$,
   (c) send vector $[\hat{\mathbf{x}}^{(k)}_\ell, \hat{\mathbf{y}}^{(\ell)}_k]$ to processor P_ℓ.
3. compute output-subvector
   (a) $\mathbf{y}^{(k)} \leftarrow \mathbf{A}^{(k)}_{kk}\mathbf{x}^{(k)}$, ▶ input-output-local tasks of P_k
   (b) $\mathbf{y}^{(k)} \leftarrow \mathbf{y}^{(k)} + \mathbf{A}^{(k)}_{k\ell}\hat{\mathbf{x}}^{(\ell)}_k$ and ▶ output-local tasks of P_k
   (c) $\mathbf{y}^{(k)} \leftarrow \mathbf{y}^{(k)} + \sum_{\ell \neq k} \hat{\mathbf{y}}^{(k)}_\ell$. ▶ input-local tasks of other processors

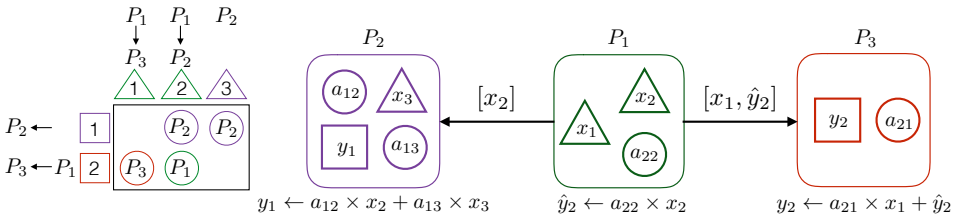

Fig. 3: An illustration of Algorithm 2 for the local fine-grain partition in Figure 2.

vector entries of $\hat{\mathbf{y}}^{(\ell)}_k$ correspond to the nonzero rows of $\mathbf{A}^{(k)}_{\ell k}$. That is, $\hat{\mathbf{x}}^{(k)}_\ell = [x_j : a_{ij} \in \mathbf{A}^{(\ell)}_{\ell k}]$ and $\hat{\mathbf{y}}^{(\ell)}_k = [\hat{y}_i : a_{ij} \in \mathbf{A}^{(k)}_{\ell k}]$. This message is heterogeneous if $\mathbf{A}^{(k)}_{\ell k}$ and $\mathbf{A}^{(\ell)}_{\ell k}$ are both nonzero and homogeneous otherwise. We also note that the number of messages is equal to the number of nonzero off-diagonal blocks of the block structure (3) of $\mathbf{A}$ induced by the vector distribution $(\Pi(\mathbf{x}), \Pi(\mathbf{y}))$. Figure 3 illustrates the steps of Algorithm 2 on the sample local fine-grain partition given in Figure 2. As seen in the figure, there are only two messages to be communicated. One message is homogeneous, which is from P_1 to P_2 and contains only an input-vector entry x_2, whereas the other message is heterogeneous, which is from P_1 to P_3 and contains an input-vector entry x_1 and a partially computed output-vector entry $\hat{y}_2$.

4. Two proposed methods for local row-column-parallel partitioning. We propose two methods to find a local row-column-parallel partition that is required for 1.5D local row-column-parallel SpMV. One method finds vector and nonzero distributions simultaneously, whereas the other one has two parts in which vector and nonzero distributions are found separately.

4.1. A directed hypergraph model for simultaneous vector and nonzero distribution. In this method, we adopt the elementary hypergraph model for the fine-grain partitioning [16] and introduce an additional locality constraint on partitioning in order to obtain a local fine-grain partition. In this hypergraph model

$\mathcal{H}_{2D} = (\mathcal{V}, \mathcal{N})$, there is an input-data vertex for each input-vector entry, an output-data vertex for each output-vector entry and a task vertex for each fine-grain task (or per matrix nonzero) for a given matrix $\mathbf{A}$. That is,

$$\mathcal{V} = \{v_x(j) : x_j \in \mathbf{x}\} \cup \{v_y(i) : y_i \in \mathbf{y}\} \cup \{v_z(ij) : a_{ij} \in \mathbf{A}\} .$$

The input- and output-data vertices have zero weights, whereas the task vertices have unit weights. In $\mathcal{H}_{2D}$, there is an input-data net for each input-vector entry, and an output-data net for each output-vector entry. An input-data net $n_x(j)$, corresponding to the input-vector entry x_j, connects all task vertices associated with the nonzeros at column j as well as the input-data vertex $v_x(j)$. Similarly, an output-data net $n_y(i)$, corresponding to the output-vector entry y_i, connects all task vertices associated with the nonzeros at row i as well as the output-data vertex $v_y(i)$. That is

$$\begin{aligned} \mathcal{N} &= \{n_x(j) : x_j \in \mathbf{x}\} \cup \{n_y(i) : y_i \in \mathbf{y}\} , \\ n_x(j) &= \{v_x(j)\} \cup \{v_z(ij) : a_{ij} \in \mathbf{A}, 1 \leq i \leq m\} , \text{ and} \\ n_y(i) &= \{v_y(i)\} \cup \{v_z(ij) : a_{ij} \in \mathbf{A}, 1 \leq j \leq n\}. \end{aligned}$$

Note that each input-data net connects a separate input-data vertex, whereas each output-data net connects a separate output-data vertex. We associate nets with their respective data vertices.

We enhance the elementary row-column-net hypergraph model by imposing directions on the nets; this is required for modeling the dependencies and their nature. Each input-data net $n_x(j)$ is directed from the input-data vertex $v_x(j)$ to the task vertices connected by $n_x(j)$, and each output-data net $n_y(i)$ is directed from the task vertices connected by $n_y(i)$ to the output-data vertex $v_y(i)$. Each task vertex $v_z(ij)$ is connected by a single input-data-net $n_x(j)$ and a single output-data-net $n_y(i)$.

In order to impose the locality in the partitioning, we introduce the following constraint for vertex partitioning on the directed hypergraph model $\mathcal{H}_{2D}$: each task vertex $v_z(ij)$ should be assigned to the part that contains either input-data vertex $v_x(j)$, or output-data vertex $v_y(i)$, or both. Figure 4a displays a sample 6×7 sparse matrix. Figure 4b illustrates the associated directed hypergraph model. Figure 4c shows a 3-way vertex partition of this directed hypergraph model satisfying the locality constraint, and Fig. 4d shows the local fine-grain partition decoded by this partition.

Instead of developing a partitioner for this particular directed hypergraph model, we propose a task-vertex amalgamation procedure which will help in meeting the described locality constraint by using a standard hypergraph partitioning tool. For this, we adopt and adapt a simple-yet-effective approach of Pelt and Bisseling [15]. In our adaptation, we amalgamate each task vertex $v_z(ij)$ into either input-data vertex $v_x(j)$ or output-data vertex $v_y(i)$ according to the number of task vertices connected by $n_x(j)$ and $n_y(i)$, respectively. That is, $v_z(ij)$ is amalgamated into $v_x(j)$ if column j has a smaller number of nonzeros than row i, and otherwise it is amalgamated into $v_y(i)$, where the ties are broken arbitrarily. The result is a reduced hypergraph that contains only the input- and output-data vertices amalgamated with the task vertices where the weight of a data vertex is equal to the number of task vertices amalgamated into that data vertex. As a result, the locality constraint on vertex partitioning of the initial directed hypergraph naturally holds on any vertex partitioning on the reduced hypergraph. It so happens that after this process, the net directions become irrelevant for partitioning, and hence one can use the standard hypergraph partitioning tools.

Figure 5 illustrates how to obtain a local fine-grain partition through the described task-vertex amalgamation procedure. In Figure 5a, the up and left arrows imply that

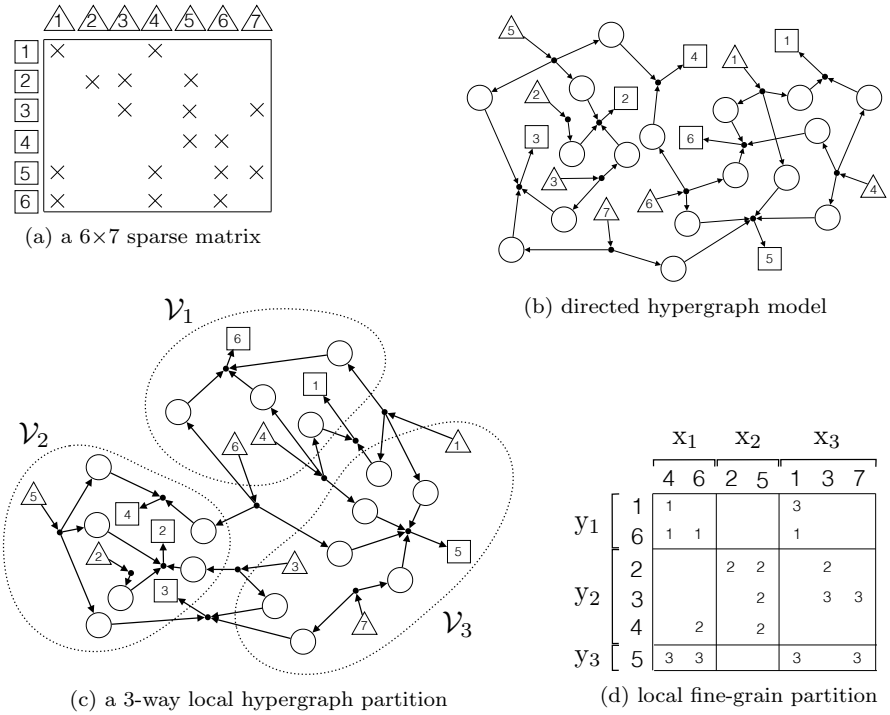

(a) a 6×7 sparse matrix

(b) directed hypergraph model

(c) a 3-way local hypergraph partition

(d) local fine-grain partition

Fig. 4: An illustration of attaining a local fine-grain partition through vertex partitioning of the directed hypergraph model that satisfies locality constraints. The input- and output-data vertices are drawn with triangles and rectangles, respectively.

a task vertex $v_z(ij)$ is amalgamated into input-data vertex $v_x(j)$ and output-data vertex $v_y(i)$, respectively. The reduced hypergraph obtained by these task-vertex amalgamations is shown in Figure 5b. Figures 5c and 5d show a 3-way vertex partition of this reduced hypergraph and the obtained local fine-grain partition, respectively. As seen in these figures, task a_{35} is assigned to processor P_2 since $v_z(3,5)$ is amalgamated into $v_x(5)$, and $v_x(5)$ is assigned to $\mathcal{V}_2$.

We emphasize here that the reduced hypergraph constructed as above is equivalent to the hypergraph model of Pelt and Bisseling [15]. In that original work, the use of this model was only for two-way partitioning (of the fine grain model) which is then used for K-way fine-grain partitioning recursively. But this distorts the locality of task vertices so that a partition obtained in further recursive steps is no more a local fine-grain partition. That is why the adaptation was necessary.

4.2. Nonzero distribution to minimize the total communication volume. This method is composed of two parts. The first parts finds a vector distribution $(\Pi(\mathbf{x}), \Pi(\mathbf{y}))$. The second part finds a nonzero/task distribution $\Pi(\mathbf{A})$ that exactly minimizes the total communication volume over all possible local fine-grain partitions which abide by $(\Pi(\mathbf{x}), \Pi(\mathbf{y}))$ of the first part. The first part can be accomplished by any conventional data partitioning method such as 1D partitioning. Therefore, this section is devoted to the second part.

Consider the block structure (3) of $\mathbf{A}$ induced by $(\Pi(\mathbf{x}), \Pi(\mathbf{y}))$. Recall that in a local fine-grain partition, due (11), the nonzero/task distribution is such that each

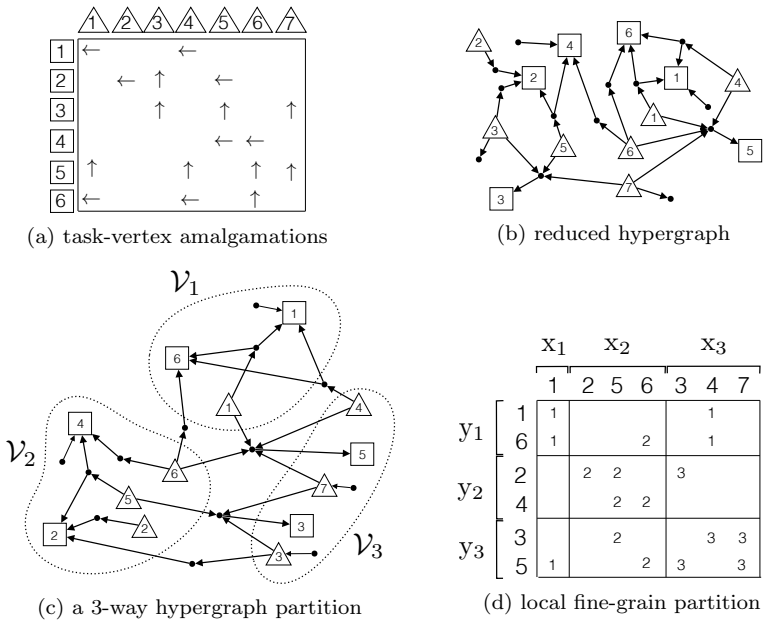

Fig. 5: An illustration of local fine-grain partitioning through task-vertex amalgamations. The input- and output-data vertices are drawn with triangles and rectangles, respectively. The figure on the bottom right shows the fine-grain partition.

diagonal block $\mathbf{A}_{kk} = \mathbf{A}_{kk}^{(k)}$, and each off-diagonal block $\mathbf{A}_{k\ell}$ is a nonzero-disjoint summation of the form $\mathbf{A}_{k\ell} = \mathbf{A}_{k\ell}^{(k)} + \mathbf{A}_{k\ell}^{(\ell)}$. This corresponds to assigning each nonzero of $\mathbf{A}_{kk}$ to P_k, for each diagonal block $\mathbf{A}_{kk}$, and assigning each nonzero of $\mathbf{A}_{k\ell}$ to either P_k or P_ℓ. Figure 6 illustrates a sample 10×12 sparse matrix and its block structure induced by a sample 3-way vector distribution which incurs four messages: from P_3 to P_1, from P_1 to P_2, from P_3 to P_2, and from P_2 to P_3 due to $\mathbf{A}_{13}$, $\mathbf{A}_{21}$, $\mathbf{A}_{23}$ and $\mathbf{A}_{32}$, respectively.

Since diagonal blocks and zero off-diagonal blocks do not incur any communication, we focus on the nonzero off-diagonal blocks. Consider a nonzero off-diagonal block $\mathbf{A}_{k\ell}$ which incurs a message from P_ℓ to P_k. The volume of this message is determined by the distribution of tasks of $\mathbf{A}_{k\ell}$ between P_k and P_ℓ. This in turn implies that distributing the tasks of each nonzero off-diagonal block can be performed independently for minimizing the total communication volume.

In the local row-column-parallel algorithm, P_ℓ sends $[\hat{\mathbf{x}}_\ell^{(k)}, \hat{\mathbf{y}}_k^{(\ell)}]$ to P_k. Here, $\hat{\mathbf{x}}_\ell^{(k)}$ corresponds to the nonzero columns of $\mathbf{A}_{\ell k}^{(\ell)}$, and $\hat{\mathbf{y}}_k^{(\ell)}$ corresponds to the nonzero rows of $\mathbf{A}_{\ell k}^{(k)}$, for a nonzero/task distribution $\mathbf{A}_{k\ell} = \mathbf{A}_{k\ell}^{(k)} + \mathbf{A}_{k\ell}^{(\ell)}$. Then, we can derive the following formula for the communication volume $\phi_{k\ell}$ from P_ℓ to P_k:

$$\phi_{k\ell} = \hat{n}(\mathbf{A}_{k\ell}^{(k)}) + \hat{m}(\mathbf{A}_{k\ell}^{(\ell)}), \tag{12}$$

where $\hat{n}(\cdot)$ and $\hat{m}(\cdot)$ refer to the number of nonzero columns and nonzero rows of the input submatrix, respectively. The total communication volume ϕ is then computed by summing the communication volumes incurred by each nonzero off-diagonal block of the block structure. Then, the problem of our interest can be described as follows.

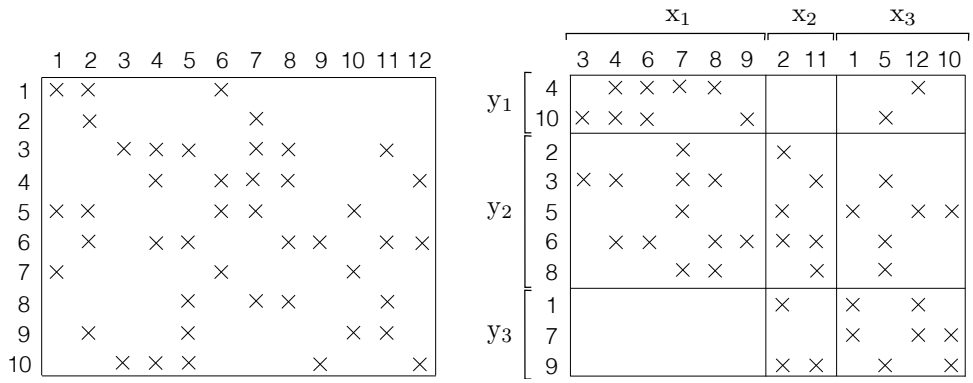

(a) a sample 10×12 sparse matrix (b) the induced block structure

Fig. 6: A sample 10×12 sparse matrix $\mathbf{A}$ and its block structure induced by input-data distribution $\Pi(\mathbf{x}) = \{\mathbf{x}^{(1)}, \mathbf{x}^{(2)}, \mathbf{x}^{(3)}\}$ and output-data distribution $\Pi(\mathbf{y}) = \{\mathbf{y}^{(1)}, \mathbf{y}^{(2)}, \mathbf{y}^{(3)}\}$, where $\mathbf{x}^{(1)} = \{x_3, x_4, x_6, x_7, x_8, x_9\}$, $\mathbf{x}^{(2)} = \{x_2, x_{11}\}$, $\mathbf{x}^{(3)} = \{x_1, x_5, x_{12}, x_{10}\}$, $\mathbf{y}^{(1)} = \{y_4, y_{10}\}$, $\mathbf{y}^{(2)} = \{y_2, y_3, y_5, y_6, y_8\}$, and $\mathbf{y}^{(3)} = \{y_1, y_7, y_9\}$.

PROBLEM 1. *Given $\mathbf{A}$ and a vector distribution $(\Pi(\mathbf{x}), \Pi(\mathbf{y}))$, find a nonzero/task distribution $\Pi(\mathbf{A})$ such that (i) each nonzero off-diagonal block has the form $\mathbf{A}_{k\ell} = \mathbf{A}_{k\ell}^{(k)} + \mathbf{A}_{k\ell}^{(\ell)}$; (ii) each diagonal block $\mathbf{A}_{kk} = \mathbf{A}_{kk}^{(k)}$ in the block structure induced by $(\Pi(\mathbf{x}), \Pi(\mathbf{y}))$; and (iii) the total communication volume $\phi = \sum_{k \neq \ell} \phi_{k\ell}$ is minimized.*

Let $G_{k\ell} = (\mathcal{U}_{k\ell} \cup \mathcal{V}_{k\ell},\ E_{k\ell})$ be the bipartite graph representation of $\mathbf{A}_{k\ell}$, where $\mathcal{U}_{k\ell}$ and $\mathcal{V}_{k\ell}$ are the set of vertices corresponding to the rows and columns of $\mathbf{A}_{k\ell}$, respectively, and $\mathcal{E}_{k\ell}$ is the set of edges corresponding to the nonzeros of $\mathbf{A}_{k\ell}$. Based on this notation, the following theorem states a correspondence between the problem of distributing nonzeros/tasks of $\mathbf{A}_{k\ell}$ to minimize the communication volume $\phi_{k\ell}$ from P_ℓ to P_k and the problem of finding a minimum vertex cover of $G_{k\ell}$. Before stating the theorem we give a brief definition of vertex covers for the sake of completeness. A subset of vertices of a graph is called *vertex cover* if each of the graph edges is incident to any of the vertices in this subset. A vertex cover is minimum if its size is the least possible. In bipartite graphs, the problem of finding a minimum vertex cover is equivalent to the problem of finding a maximum matching [13]. Aschraft and Liu [1] describe a similar application of vertex covers.

THEOREM 1. *Let $\mathbf{A}_{k\ell}$ be a nonzero off-diagonal block and $G_{k\ell} = (\mathcal{U}_{k\ell} \cup \mathcal{V}_{k\ell}, \mathcal{E}_{k\ell})$ be its bipartite graph representation.*

1. *For any vertex cover $S_{k\ell}$ of $G_{k\ell}$, there is a nonzero distribution $\mathbf{A}_{k\ell} = \mathbf{A}_{k\ell}^{(k)} + \mathbf{A}_{k\ell}^{(\ell)}$ such that $|S_{k\ell}| \geq \hat{n}(\mathbf{A}_{k\ell}^{(k)}) + \hat{m}(\mathbf{A}_{k\ell}^{(\ell)})$,*
2. *For any nonzero distribution $\mathbf{A}_{k\ell} = \mathbf{A}_{k\ell}^{(k)} + \mathbf{A}_{k\ell}^{(\ell)}$, there is a vertex cover $S_{k\ell}$ of $G_{k\ell}$ such that $|S_{k\ell}| = \hat{n}(\mathbf{A}_{k\ell}^{(k)}) + \hat{m}(\mathbf{A}_{k\ell}^{(\ell)})$.*

Proof. We prove the two parts of the theorem separately.
1) Take any vertex cover $S_{k\ell}$ of $G_{k\ell}$. Consider any nonzero distribution $\mathbf{A}_{k\ell} =$

$\mathbf{A}_{k\ell}^{(k)} + \mathbf{A}_{k\ell}^{(\ell)}$ such that

$$a_{ij} \in \begin{cases} \mathbf{A}_{k\ell}^{(k)} & \text{if } v_j \in S_{k\ell} \text{ and } u_i \notin S_{k\ell}, \\ \mathbf{A}_{k\ell}^{(\ell)} & \text{if } v_j \notin S_{k\ell} \text{ and } u_i \in S_{k\ell}, \\ \mathbf{A}_{k\ell}^{(k)} \text{ or } \mathbf{A}_{k\ell}^{(\ell)} & \text{if } v_j \in S_{\ell} \text{ and } u_i \in S_{k\ell}. \end{cases} \tag{13}$$

Since $v_j \in S_{k\ell}$ for every $a_{ij} \in \mathbf{A}_{k\ell}^{(k)}$ and $u_i \in S_{k\ell}$ for every $a_{ij} \in \mathbf{A}_{k\ell}^{(\ell)}$, $|S_{k\ell} \cap \mathcal{V}_{k\ell}| \geq \hat{n}(\mathbf{A}_{k\ell}^{(k)})$ and $|S_{k\ell} \cap \mathcal{U}_{k\ell}| \geq \hat{m}(\mathbf{A}_{k\ell}^{(\ell)})$, which in turn leads to

$$|S_{k\ell}| \geq \hat{n}(\mathbf{A}_{k\ell}^{(k)}) + \hat{m}(\mathbf{A}_{k\ell}^{(\ell)}). \tag{14}$$

2) Take any nonzero distribution $\mathbf{A}_{k\ell} = \mathbf{A}_{k\ell}^{(k)} + \mathbf{A}_{k\ell}^{(\ell)}$. Consider $S_{k\ell} = \{u_i \in U_{k\ell} : a_{ij} \in \mathbf{A}_{k\ell}^{(\ell)}\} \cup \{v_j \in V_{k\ell} : a_{ij} \in \mathbf{A}_{k\ell}^{(k)}\}$ where $|S_{k\ell}| = \hat{n}(\mathbf{A}_{k\ell}^{(k)}) + \hat{m}(\mathbf{A}_{k\ell}^{(\ell)})$. Now, consider a nonzero $a_{ij} \in \mathbf{A}_{k\ell}$ and its corresponding edge $\{u_i, v_j\} \in \mathcal{E}_{k\ell}$. If $a_{ij} \in \mathbf{A}_{k\ell}^{(k)}$, then $v_j \in S_{k\ell}$. Otherwise, $u_i \in S_{k\ell}$ since $a_{ij} \in \mathbf{A}_{k\ell}^{(\ell)}$. So, $S_{k\ell}$ is a vertex cover of $G_{k\ell}$. ∎

At this point, however, it is still not clear how the reduction from the problem of distributing the nonzeros/tasks to the problem of finding the minimum vertex cover holds. For this purpose, using Theorem 1, we show that a minimum vertex cover of $G_{k\ell}$ can be decoded as a nonzero distribution of $\mathbf{A}_{k\ell}$ with the minimum communication volume $\phi_{k\ell}$ as follows. Let $S_{k\ell}^*$ be a minimum vertex cover of $G_{k\ell}$ and $\phi_{k\ell}^*$ be the minimum communication volume incurred by a nonzero/task distribution of $\mathbf{A}_{k\ell}$. Then, $|S_{k\ell}^*| = \phi_{k\ell}^*$, since the first and second parts of Theorem 1 imply $|S_{k\ell}^*| \geq \phi_{k\ell}^*$ and $|S_{k\ell}^*| \leq \phi_{k\ell}^*$, respectively. We decode an optimal nonzero/task distribution $\mathbf{A}_{k\ell} = \mathbf{A}_{k\ell}^{(k)} + \mathbf{A}_{k\ell}^{(\ell)}$ out of $S_{k\ell}^*$ according to (13) where one such distribution is

$$\mathbf{A}_{k\ell}^{(k)} = \{a_{ij} \in \mathbf{A}_{k\ell} : v_j \in S_{k\ell}^*\} \text{ and } \mathbf{A}_{k\ell}^{(\ell)} = \{a_{ij} \in \mathbf{A}_{k\ell} : v_j \notin S_{k\ell}^*\}. \tag{15}$$

Let $\phi_{k\ell}$ be the communication volume incurred by this nonzero/task distribution. Then, $|S_{k\ell}^*| \geq \phi_{k\ell}$ due to (14), and $\phi_{k\ell} = \phi_{k\ell}^*$ since $\phi_{k\ell}^* = |S_{k\ell}^*| \geq \phi_{k\ell} \geq \phi_{k\ell}^*$.

Figure 7 illustrates the reduction on a sample 5×6 nonzero off-diagonal block $\mathbf{A}_{k\ell}$. The left side and middle of this figure respectively display $\mathbf{A}_{k\ell}$ and its bipartite graph representation $G_{k\ell}$, which contains 5 row vertices and 6 column vertices. On the middle of the figure, a minimum vertex cover $S_{k\ell}$ that contains two row vertices $\{u_3, u_6\}$ and two column vertices $\{v_7, v_8\}$ is also shown. The right side of the figure displays how this minimum vertex cover is decoded as a nonzero/task distribution $\mathbf{A}_{k\ell} = \mathbf{A}_{k\ell}^{(k)} + \mathbf{A}_{k\ell}^{(\ell)}$. As a result of this decoding, P_ℓ sends $[x_7, x_8, \hat{y}_3, \hat{y}_6]$ to P_k in a single message. Note that a nonzero corresponding to an edge connecting two cover vertices can be assigned to either $\mathbf{A}_{k\ell}^{(k)}$ or $\mathbf{A}_{k\ell}^{(\ell)}$ without changing the communication volume from P_ℓ to P_k. The only change that may occur is in the values of partially computed output-vector entries to be communicated. For instance, in the figure, nonzero a_{37} is assigned to $\mathbf{A}_{k\ell}^{(k)}$. Since both u_3 and v_7 are cover vertices, a_{37} could be assigned to $\mathbf{A}_{k\ell}^{(\ell)}$ with no change in the communicated entries but the value of $\hat{y}_3$.

Algorithm 3 gives a sketch of our method to find a nonzero/task distribution that minimizes the total communication volume based on Theorem 1. For each nonzero off-diagonal block $\mathbf{A}_{k\ell}$, the algorithm first constructs $G_{k\ell}$, then obtains a minimum vertex cover $S_{k\ell}$, and then decodes $S_{k\ell}$ as a nonzero/task distribution $\mathbf{A}_{k\ell} = \mathbf{A}_{k\ell}^{(k)} + \mathbf{A}_{k\ell}^{(\ell)}$ according to (15). Hence, the communication volume incurred by $\mathbf{A}_{k\ell}$ is equal to the size of the cover $|S_{k\ell}|$. In detail, each row vertex u_i on the cover incurs an output

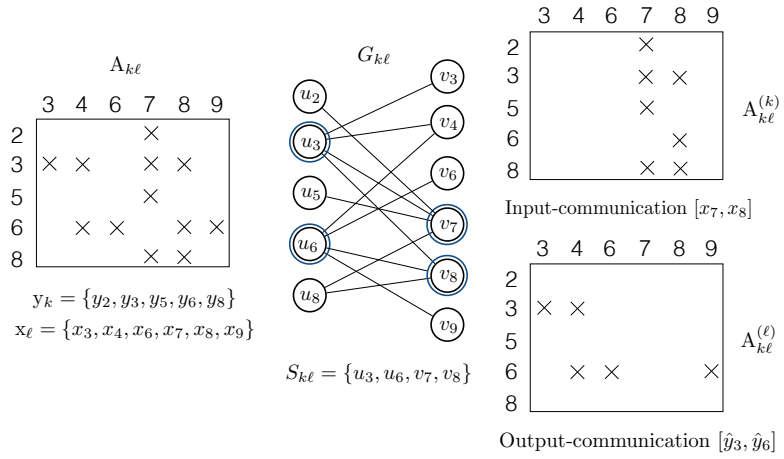

Fig. 7: The minimum vertex cover model for minimizing the communication volume $\phi_{k\ell}$ from P_ℓ to P_k. According to the vertex cover $S_{k\ell}$, P_ℓ sends $[x_7, x_8, \hat{y}_3, \hat{y}_6]$ to P_k.

communication of $\hat{y}_i \in \hat{\mathbf{y}}_\ell^{(k)}$, and each column vertex v_j on the cover incurs an input communication of $x_j \in \hat{\mathbf{x}}_k^{(\ell)}$. We recall that P_ℓ sends $\hat{\mathbf{y}}_\ell^{(k)}$ and $\hat{\mathbf{x}}_k^{(\ell)}$ to P_k in a single message in the proposed row-column-parallel sparse matrix-vector multiply algorithm.

Algorithm 3 Nonzero/task distribution to minimize the total communication volume

```
1: procedure NonzeroTaskDistributeVolume(A, Π(x), Π(y))
2:     for each nonzero off-diagonal block A_kℓ do                ▶ See (3)
3:         Construct G_kℓ = (U_kℓ ∪ V_kℓ, E_kℓ)        ▶ Bipartite graph representation
4:         S_kℓ ← MinimumVertexCover(G_kℓ)
5:         for each nonzero a_ij ∈ A_kℓ do
6:             if v_j ∈ S_kℓ then        ▶ v_j ∈ V_kℓ is a column vertex and v_j ∈ S_kℓ
7:                 A_kℓ^(k) ← A_kℓ^(k) ∪ {a_ij}
8:             else                      ▶ u_i ∈ U_kℓ is a row vertex and u_i ∈ S_kℓ
9:                 A_kℓ^(ℓ) ← A_kℓ^(ℓ) ∪ {a_ij}
```

Figure 8 illustrates the steps of Algorithm 3 on the block structure given in Figure 6b. Figure 8a shows four bipartite graphs each corresponding to a nonzero off-diagonal block. In this figure, a minimum vertex cover for each bipartite graph is also shown. Figure 8b illustrates how to decode a local fine-grain partition from those minimum vertex covers. In this figure, the nonzeros are represented with the processor to which they are assigned. As seen in the figure, the number of entries sent from P_1 to P_2 is four, that is, $\phi_{21} = 4$, and the number of entries sent from P_3 to P_1, from P_3 to P_2 and from P_2 to P_3 are all two, that is, $\phi_{13} = \phi_{23} = \phi_{32} = 2$.

We note here that the objective of this method is to minimize the total communication volume under a given vector distribution. Since blocks of nonzeros are assigned, a strict load balance cannot be always maintained.

5. Related work. Here we review recent related work on matrix partitioning for parallel SpMV.

Kuhlemann and Vassilevski [14] recognize the need to reduce the number of messages in parallel sparse matrix vector multiply operations with matrices corresponding

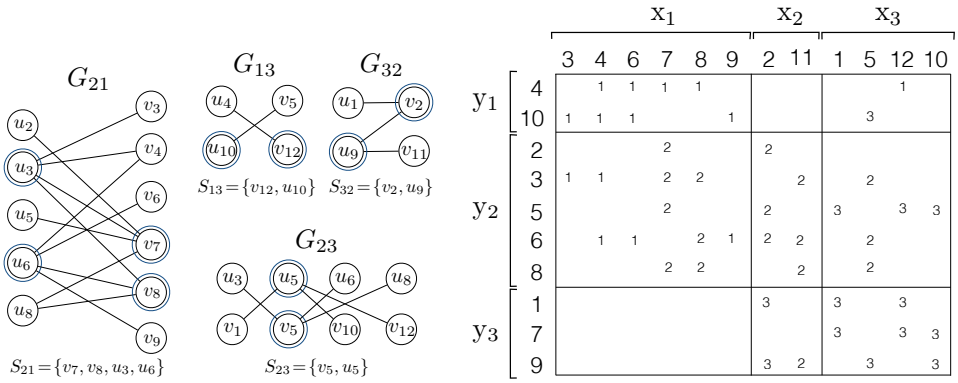

(a) a minimum vertex cover for each nonzero off-diagonal block of Figure 6b.

(b) a local fine-grain partition attained by optimal nonzero/task distribution.

Fig. 8: An optimal nonzero distribution minimizing the total communication volume obtained by Algorithm 3. The matrix nonzeros are represented with the processors they are assigned to. The total communication volume is 10, where P_1 sends $[x_7, x_8, \hat{y}_3, \hat{y}_6]$ to P_2; P_3 sends $[x_{12}, \hat{y}_{10}]$ to P_1; P_3 sends $[x_2, \hat{y}_9]$ to P_1; and P_3 sends $[x_5, \hat{y}_5]$ to P_2.

to scale-free graphs. They present methods to embed the given graph in a bigger one to reduce the number of messages. The gist of the method is to split a vertex into a number of copies (the number is determined with a simple calculation to limit the maximum number of messages per processor). In such a setting, the SpMV operations with the matrix associated with the original graph, $\mathbf{y} \leftarrow \mathbf{A}\mathbf{x}$, is then cast as triple sparse matrix vector products of the form $\mathbf{y} \leftarrow \mathbf{Q}^T(\mathbf{B}(\mathbf{Q}\mathbf{x}))$. This original work can be extended to other matrices (not necessarily symmetric, nor square) by recognizing the triplet product as a communication on $\mathbf{x}$ for duplication (for the columns that are split), communication of $\mathbf{x}$ vector entries (duplicates are associated with different destinations), multiplication, and as a communication on the output vector (for the rows that are split) to gather results. This exciting extension requires further analysis.

Boman et al. [2] propose a 2D partitioning method obtained by post-processing a 1D partition. Given a 1D partition among P processors, the method maps the $P \times P$ block structure to a virtual mesh of size $P_r \times P_c$ and reassigns the off-diagonal blocks so as to limit the number of messages per processor by $P_r + P_c$. The post-processing is fast, and hence the method is as nearly efficient as a 1D partitioning method. However, the communication volume and the computational load balance obtained in the 1D partitioning phase are disturbed and the method does not have any means to control the perturbation. The proposed two-part method (Section 4.2), is similar to this work in this aspect; a strict balance cannot always be achieved; yet a finer approach is discussed in the preliminary version of the paper [12].

Pelt and Bisseling [15] propose a model to partition sparse matrices into two parts (which then can be used recursively to partition into any number of parts). The essential idea has two steps. First, the nonzeros of a given matrix $\mathbf{A}$ are split into two different matrices (of the same size as the original matrix), say $\mathbf{A} = \mathbf{A}_r + \mathbf{A}_c$. Second, $\mathbf{A}_r$ and $\mathbf{A}_c$ are partitioned together, where $\mathbf{A}_r$ is partitioned rowwise, and $\mathbf{A}_c$ is partitioned columnwise. As all nonzeros of $\mathbf{A}$ are in only one of $\mathbf{A}_r$ or $\mathbf{A}_c$, the final result is a two-way partitioning of the nonzeros of $\mathbf{A}$. The resulting partition on

A achieves load balance and reduces the total communication volume by the standard hypergraph partitioning techniques.

Two-dimensional partitioning methods that bound the maximum number of messages per processor, such as the checkerboard [5, 8] and orthogonal recursive bisection [17] based methods, have been used in modern applications [18, 20], sometimes without graph/hypergraph partitioning [19]. In almost all cases, inadequacy of 1D partitioning schemes are confirmed.

All previous work (including those that were summarized above) assumes the standard SpMV algorithm based on expanding **x**-vector entries, performing multiplies with matrix entries, and folding **y**-vector entries. Compared to all these previous work, ours has therefore a distinctive characteristic. In this work, we introduce the novel concept of heterogeneous messages where **x**-vector and partially computed **y**-vector entries are possibly communicated within the same message packet. In order to make use of this, we search for a special 2D partition on the matrix nonzeros in which a nonzero is assigned to a processor holding either the associated input-vector entry, or the associated output-vector entry, or both. The implication is that the proposed local row-column-parallel SpMV algorithm requires only a single communication phase (all the previous algorithms based on 2D partitions require two communication phases) as is the case for the parallel algorithms based on 1D partitions; yet the proposed algorithm achieves a greater flexibility to reduce the communication volume than the 1D methods.

6. Experiments. We performed our experiments on a large selection of sparse matrices obtained from the University of Florida (UFL) sparse matrix collection [9]. We used square and structurally symmetric matrices with 500–10M nonzeros. At the time of experiments, we had 904 such matrices. We discarded 14 matrices as they contain diagonal entries only, and we also excluded one matrix (`kron_g500-logn16`) because it took extremely long to have a partition with the hypergraph partitioning tool used in the experiments. We conducted our experiments for $K = 64$ and $K = 1024$ and omit the cases when the number of rows is less than $50 \times K$. As a result, we had 566 and 168 matrices for the experiments with $K = 64$ and 1024, respectively. We separate all our test matrices into two groups according to the maximum number of nonzeros per row/column, more precisely, according to whether the test matrix contains a dense row/column or not. We say a row/column dense if it contains at least $10\sqrt{m}$ nonzeros, where m denotes the number of rows/columns. Hence, for $K = 64$ and 1024, the first group respectively contains 477 and 142 matrices that have no dense rows/columns out of 566 and 168 test matrices. The second group contains the remaining 89 and 26 matrices, each having some dense rows/column, for $K = 64$ and 1024, respectively.

In the experiments, we evaluated the partitioning qualities of the local fine-grain partitioning methods proposed in Section 4 against 1D rowwise (`1D-H` [3]), the 2D fine-grain (`2D-H` [4]), and two checkerboard partitioning methods (`2D-B` [2], `2D-C` [5]). For the method proposed in Section 4.1, we obtain a local fine-grain partition through the directed hypergraph model (`1.5D-H`) using the procedure described at the end of that subsection. For the method proposed in Section 4.2 (`1.5D-V`), the required vector distribution is obtained by 1D rowwise partitioning using the column-net hypergraph model. Then, we obtain a local fine-grain partition on this vector distribution with a nonzero/task distribution that minimizes the total communication volume.

The `1D-H`, `2D-H`, `2D-C` and `1.5D-H` methods are based on hypergraph models. Although all these models allow arbitrary distribution of the input- and output-vectors,

in the experiments, we consider conformal partitioning of input and output vectors, by using vertex amalgamation of the input- and output-vector entries [16]. We used PaToH [3, 6] with default parameters where the maximum allowable imbalance ratio is 3% for partitioning. We also notice that the `1.5D-V` and `2D-B` methods are based on `1D-H` and keeps the vector distribution obtained from `1D-H` intact. Hence, in the experiments, the input and output vectors for those methods are conformal as well. Finally, since PaToH depends on randomization, we report the geometric mean of ten different runs for each partitioning instance.

In all experiments, we report the results using performance profiles [10] which is very helpful in comparing multiple methods over a large collection of test cases. In a performance profile, we compare methods according to the best performing method for each test case and measure in what fraction of the test cases a method performs within a factor of the best observed performance. For example, a point (abscissa = 1.05, ordinate = 0.30) on the performance curve of a given method refers to the fact that for 30% of the test cases, the method performs within a factor of 1.05 of the best observed performance. As a result, a method that is closer to top-left corner is better. In the load balancing performance profiles displayed in Figures 9b, 9d, 10b and 10d, we compare performance results with respect to the performance of perfect balance instead best observed performance. That is, a point (abscissa = 6% and ordinate = 0.40) on the performance curve of a given method means that for 40% of the test cases, the method produces a load imbalance ratio less than or equal to 6%.

Figures 9 and 10 both display performance profiles of four task-and-data distribution methodsin terms of the total communication volume and the computational load imbalance. Figure 9 displays performance profiles for the set of matrices with no dense rows/columns, whereas Figure 10 displays performance profiles for the set of matrices containing dense rows/columns.

As seen in Figure 9, for the set of matrices with no dense rows/columns, the relative performances of all methods are similar for $K = 64$ and $K = 1024$ in terms of both communication volume and load imbalance. As seen in Figures 9a and 9c, all methods except the `1.5D-H` method achieve a total communication volume at most 30% more than the best in almost 80% of the cases in this set of matrices. As seen in these two figures, the proposed `1.5D-V` method performs significantly better than all other methods, whereas the `2D-H` method is the second best performing method. As also seen in the figures, `1D-H` displays the third best performance, whereas `1.5D-H` shows the worst performance. As seen in Figures 9b and 9d, in terms of load balance, the `2D-H` method is the best performing method. As also seen in the figures, the proposed `1.5D-V` method displays considerably worse performance than the others. Specifically, all methods except `1.5D-V` achieve a load imbalance below 3% in almost all test cases. In terms of the total communication volume, 2D checkerboard partitioning methods perform considerably worse than `1.5D-V`, `2D-H` and `1D-H` methods. The first alternative `2D-B` obtains better results than `2D-C`. For load balance, `2D-C` behaves similar to `1D-H`, `2D-H` and `1.5D-H` methods except that `2D-C` achieves a load imbalance below 5% (instead of 3%) for almost all instances. `2D-B` behaves similar to `1.5D-V`, and does not achieve a good load balance.

As seen in Figure 10, for the set of matrices with some dense rows/columns, all methods display a similar performance for $K = 64$ and $K = 1024$ in terms of the total communication volume. As in the previous dataset, in terms of the total communication volume, the `1.5D-V` and `2D-H` methods are again the best and second best methods, respectively, as seen in Figures 10a and 10c. As also seen in these figures, `1.5D-H` is the third best performing method in terms of the total communication vol-

Method	SpMV	Partitioning	Method
1D-H	row-parallel	rowwise	[2]
2D-H	row-column-parallel	fine-grain	[3]
2D-B	row-column-parallel	checker-board	[1]
2D-C	row-column-parallel	checker-board	[4]
1.5D-H	local row-column-parallel	local fine-grain	§4.1
1.5D-V	local row-column-parallel	local fine-grain	§4.2

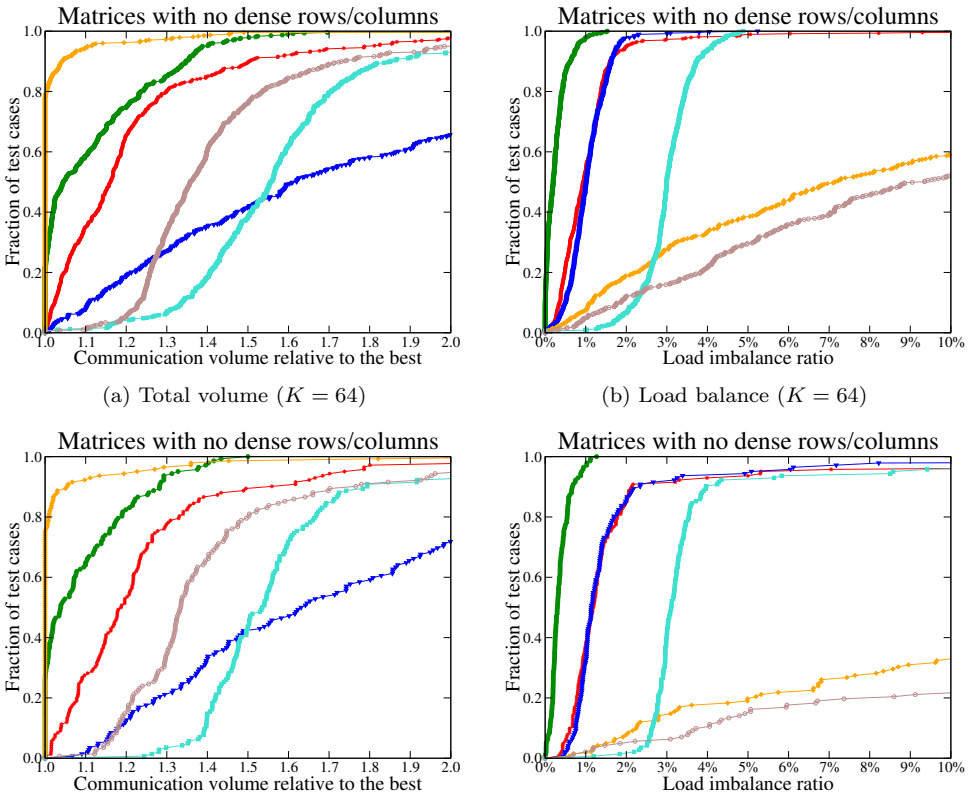

(a) Total volume ($K = 64$)

(b) Load balance ($K = 64$)

(c) Total communication volume ($K = 1024$)

(d) Load balance ($K = 1024$)

Fig. 9: Performance profiles comparing the total communication volume and load balance using test matrices with no dense rows/columns for $K = 64$ and 1024.

ume, whereas 1D-H shows considerably worse performance. The 2D-H method achieves near-to-perfect load balance in almost all cases, as seen in Figures 10b and 10d. As also seen in these figures, the 1.5D-H method displays a load imbalance lower than approximately 6% and 14% for all test matrices for $K = 64$ and 1024, respectively. This shows the success of the vertex amalgamation procedure within the context of the directed hypergraph model described in Section 4.1. As seen in Figure 10c, the total communication volume does not exceed the best method by 40% in about 75% and 85% of the test cases for the 1.5D-H and 2D-H methods, respectively, for $K = 1024$. The two 2D checkerboard methods display considerably worse performance than the others (except 1D-H, which also shows a poor performance) in terms of the total communication volume. When $K = 64$, 2D-C shows an acceptable performance however when $K = 1024$ its performance considerably deteriorates in terms of load balance. 2D-B obtains worse results. This not surprising since 2D-B is a modification of 1D-H

Method	SpMV	Partitioning	Method
1D-H	row-parallel	rowwise	[2]
2D-H	row-column-parallel	fine-grain	[3]
2D-B	row-column-parallel	checker-board	[1]
2D-C	row-column-parallel	checker-board	[4]
1.5D-H	local row-column-parallel	local fine-grain	§4.1
1.5D-V	local row-column-parallel	local fine-grain	§4.2

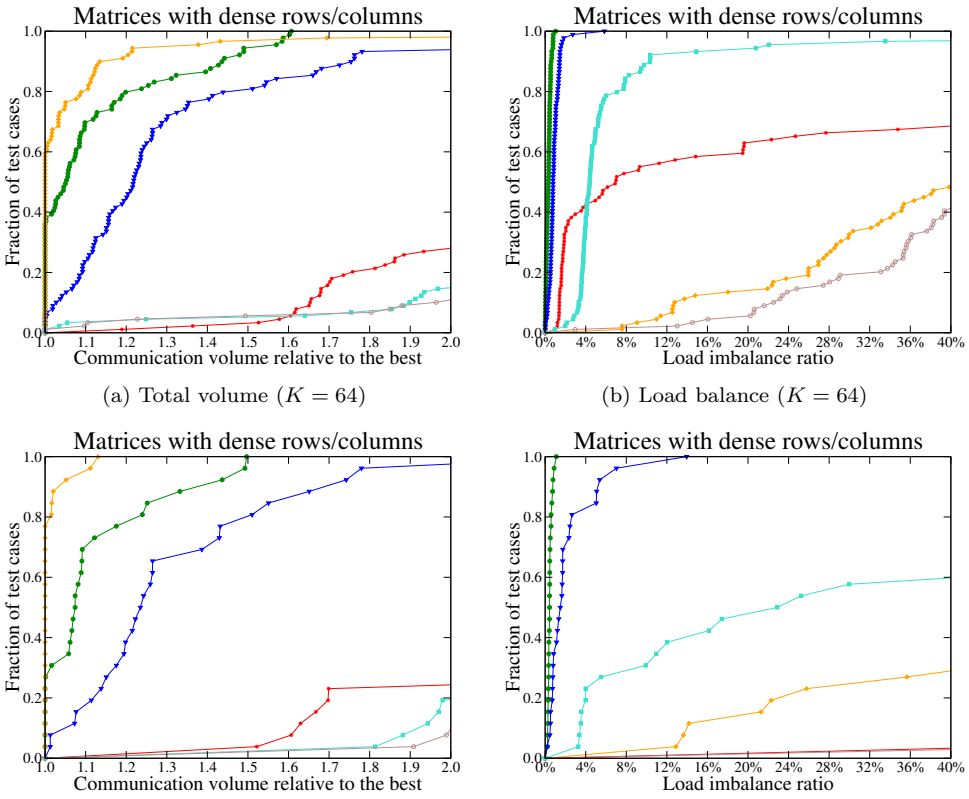

(a) Total volume ($K = 64$)

(b) Load balance ($K = 64$)

(c) Total communication volume ($K = 1024$)

(d) Load balance ($K = 1024$)

Fig. 10: Performance profiles comparing the total communication volume and the load balance on test matrices with dense rows/columns for $K = 64$ and 1024.

whose load balance performance is already very poor.

Figures 11a and 11b compare the methods in terms of the total and maximum message counts, respectively, using all test matrices for $K = 1024$. We note that these are secondary metrics and none of the methods addresses them explicitly as the main objective function. Since 1.5D-V uses the conformal distribution of the input- and output-vectors obtained from 1D-H, the total and the maximum message count of 1.5D-V are equivalent to those of 1D-H in these experiments. As seen in the figures, in terms of the total and the maximum message counts, 2D-B, 2D-C and 1D-H (also 1.5D-V) display the best performance, 2D-H performs considerably poor and 1.5D-H performs in between. At a finer look, the method 2D-B is the winner with both metrics. 1.5D-V (as 1D-H) and the other checkerboard method 2D-C follows it, where 2D checkerboard methods show clearer advantage.

Figure 11c compares all four methods in terms of the maximum communication

volume sent from a processor for $K = 1024$. The 1.5D-V method performs significantly better than all others, 2D-H is the second best performing method, 1D displays the third best, and 1.5D-H displays the worst performance. These relative performances of the methods in terms of the maximum communication volume resemble their relative performances in terms of the total communication volume as expected.

Figure 11d compares the methods in terms of partitioning times for $K = 1024$. The run time of the 1.5D-V method involves the time spent for obtaining the vector distribution, which is the run time of the 1D-H method in our case. As seen in the figure, the 1D-H, 1.5D-V and 1.5D-H methods display comparable performances, whereas the 2D-H method takes significantly longer. The longer run time of 2D-H stems from the large size of the hypergraph model. 2D-B displays comparable performance (in terms of running-time) with that of 1D-H, 1.5D-V and 1.5D-H methods. Meanwhile, 2D-C is considerably slower than all others except 2D-H.

In summary, the 1.5D-H method is a promising alternative for sparse matrices with dense rows/columns. It obtaines a total communication volume close to 2D-H, near-perfect balance, considerably lower message count than 2D-H, and has short partitioning time. The 1.5D-V method performs at the extremes: the best for the total communication volume, and the worst for the load balance, especially for matrices with dense rows/columns. Nevertheless, 1.5D-V could still be favorable to other methods for particular matrices due to lower communication volume. In short, if a sparse matrix contains dense rows/columns, then 1.5D-H seems to be the method of choice in general; otherwise, 1.5D-V and 1D-H are reasonable alternatives competing with each other. The 2D checkerboard based methods perform worse than the 1.5D methods, but they have good performance in terms of the message count based metrics. In particular, 2D-B is a fast method with a striking performance in reducing the latency, but load balance can be an issue. These could be deciding factors for large scale systems. On the other hand, 2D-C obtains better balance than 2D-B, but is slower.

7. Conclusion and further discussions. This paper introduced 1.5D parallelism for the sparse matrix-vector multiply (SpMV) operations. We presented the local row-column parallel SpMV that uses this novel parallelism. This multiply algorithm is the fourth one in the literature for SpMV in addition to the well-known 1D row-parallel, 1D column-parallel and 2D row-column-parallel ones. In this paper, we also proposed two methods (1.5D-H and 1.5D-V) to distribute tasks and data in accordance with the requirements of the proposed 1.5D parallel algorithm. Using a large set of matrices from the UFL sparse matrix collection, we compared the partitioning qualities of these two methods against the standard 1D and 2D methods.

The experiments suggest the use of the local row-column-parallel SpMV with a local fine-grain partition obtained by the proposed directed hypergraph model for matrices with dense rows/columns. This is because the performance of the proposed 1.5D partitioning is close to that of 2D fine-grain partitioning (2D-H) in terms of the partitioning quality, with considerably less number of messages and much faster execution.

We considered the problem mainly from a theoretical point of interest and leave the performance of 1.5D parallel SpMV algorithms in terms of the parallel multiply timings as a future work. We note that the main ideas behind the proposed 1.5D parallelism, such as heterogeneous messaging and avoiding nonlocal tasks by a locality constraint on partitioning, are of course not restricted to the parallel SpMV operation and these ideas can be extended to other parallel computations as well.

Method	SpMV	Partitioning	Method
1D-H	row-parallel	rowwise	[2]
2D-H	row-column-parallel	fine-grain	[3]
2D-B	row-column-parallel	checker-board	[1]
2D-C	row-column-parallel	checker-board	[4]
1.5D-H	local row-column-parallel	local fine-grain	§4.1
1.5D-V	local row-column-parallel	local fine-grain	§4.2

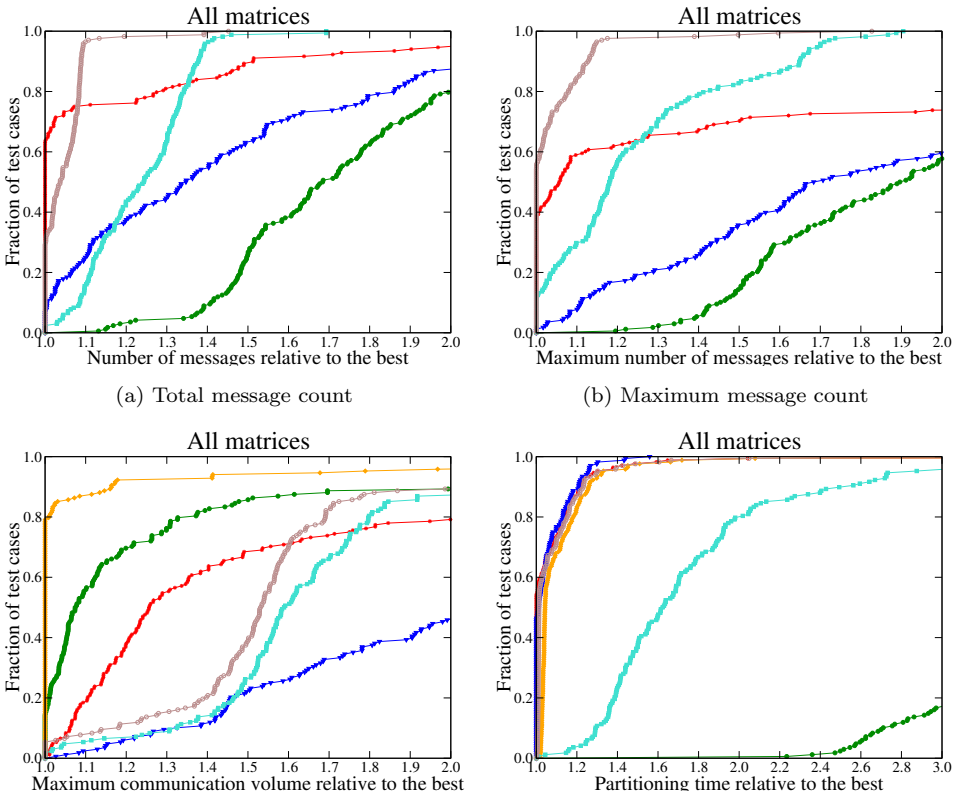

(a) Total message count (b) Maximum message count

(c) Maximum volume (d) Partitioning time

Fig. 11: Performance profiles comparing the total message count and the maximum message count for three methods 1D-H, 2D-H and 1.5D-H, maximum communication volume per processor and partitioning time for all methods on all test matrices for $K = 1024$. In 11a and 11b, 1.5D-V's profiles are identical to that of 1D-H, and hence not shown.

REFERENCES

[1] C. Ashcraft and J. W. H. Liu, *Applications of the Dulmage-Mendelsohn decomposition and network flow to graph bisection improvement*, SIAM Journal on Matrix Analysis and Applications, 19 (1998), pp. 325–354.

[2] E. G. Boman, K. D. Devine, and S. Rajamanickam, *Scalable matrix computations on large scale-free graphs using 2d graph partitioning*, in Proceedings of the International Conference on High Performance Computing, Networking, Storage and Analysis, SC '13, New York, NY, USA, 2013, ACM, pp. 50:1–50:12.

[3] Ü. Çatalyürek and C. Aykanat, *Hypergraph-partitioning-based decomposition for parallel sparse-matrix vector multiplication*, Parallel and Distributed Systems, IEEE Transactions on, 10 (1999), pp. 673–693.

[4] Ü. Çatalyürek and C. Aykanat, *A fine-grain hypergraph model for 2d decomposition of sparse matrices*, Parallel and Distributed Processing Symposium, International, 3 (2001), p. 30118b.
[5] Ü. Çatalyürek and C. Aykanat, *A hypergraph-partitioning approach for coarse-grain decomposition*, in Supercomputing, ACM/IEEE 2001 Conference, IEEE, 2001, pp. 42–42.
[6] Ü. Çatalyürek and C. Aykanat, *Patoh (partitioning tool for hypergraphs)*, in Encyclopedia of Parallel Computing, Springer, 2011, pp. 1479–1487.
[7] Ü. Çatalyürek, C. Aykanat, and B. Uçar, *On two-dimensional sparse matrix partitioning: Models, methods, and a recipe*, SIAM Journal on Scientific Computing, 32 (2010), pp. 656–683.
[8] Ü. V. Çatalyürek, C. Aykanat, and B. Uçar, *On two-dimensional sparse matrix partitioning: Models, methods, and a recipe*, SIAM J. Sci. Comput., 32 (2010), pp. 656–683.
[9] T. A. Davis and Y. Hu, *The University of Florida sparse matrix collection*, ACM Trans. Math. Softw., 38 (2011), pp. 1:1–1:25.
[10] E. D. Dolan and J. J. Moré, *Benchmarking optimization software with performance profiles*, Mathematical programming, 91 (2002), pp. 201–213.
[11] K. Kaya, B. Uçar, and U. V. Çatalyürek, *Analysis of partitioning models and metrics in parallel sparse matrix-vector multiplication*, in Parallel Processing and Applied Mathematics (PPAM2014), R. Wyrzykowski, J. Dongarra, K. Karczewski, and J. Waśniewski, eds., Lecture Notes in Computer Science, Warsaw, Poland, 2014, Springer Berlin Heidelberg, pp. 174–184.
[12] E. Kayaaslan, B. Uçar, and C. Aykanat, *Semi-two-dimensional partitioning for parallel sparse matrix-vector multiplication*, in Parallel and Distributed Processing Symposium Workshop (IPDPSW), 2015 IEEE International, IEEE, 2015, pp. 1125–1134.
[13] D. Konig, *Gráfok és mátrixok. matematikai és fizikai lapok, 38: 116–119, 1931.*
[14] V. Kuhlemann and P. S. Vassilevski, *Improving the communication pattern in matrix-vector operations for large scale-free graphs by disaggregation*, SIAM Journal on Scientific Computing, 35 (2013), pp. S465–S486.
[15] D. M. Pelt and R. H. Bisseling, *A medium-grain method for fast 2d bipartitioning of sparse matrices*, in Parallel and Distributed Processing Symposium, 2014 IEEE 28th International, IEEE, 2014, pp. 529–539.
[16] B. Uçar and C. Aykanat, *Revisiting hypergraph models for sparse matrix partitioning*, SIAM review, 49 (2007), pp. 595–603.
[17] B. Vastenhouw and R. H. Bisseling, *A two-dimensional data distribution method for parallel sparse matrix-vector multiplication*, SIAM Review, 47 (2005), pp. 67–95.
[18] R. S. Xin, J. E. Gonzalez, M. J. Franklin, and I. Stoica, *Graphx: A resilient distributed graph system on spark*, in First International Workshop on Graph Data Management Experiences and Systems, GRADES '13, New York, NY, USA, 2013, ACM, pp. 2:1–2:6.
[19] A. Yoo, A. H. Baker, R. Pearce, and V. E. Henson, *A scalable eigensolver for large scale-free graphs using 2D graph partitioning*, in Proc. International Conference for High Performance Computing, Networking, Storage and Analysis, ACM, 2011, pp. 63:1–63:11.
[20] A. Yoo, E. Chow, K. Henderson, W. McLendon, B. Hendrickson, and U. Catalyurek, *A scalable distributed parallel breadth-first search algorithm on bluegene/l*, in Proceedings of the 2005 ACM/IEEE Conference on Supercomputing, SC '05, Washington, DC, USA, 2005, IEEE Computer Society, p. 25.